Proceedings of the 2014 IEEE
International Conference on Robotics and Biomimetics
December 5-10, 2014, Bali, Indonesia

Strategies, Controllers, and Coordination: Bi-Manual Snap Assembly Automation.

Juan Rojas, TianQiang Guan, Weiqiang Luo
School of Software
Sun Yat Sen University
Guangzhou, Guangdong, 510006, China

Kensuke Harada.
Intelligent Sys. Research Institute, AIST
Tsukuba, Ibaraki, 305-8568, Japan

***Abstract*— In robotic manipulation, higher levels of dexterity are sought in multiple domains. More unstructured environments demand that robots are able to dexterously and flexibly resolve their tasks. Dual-arm humanoid robots are seen as advantageous for such tasks. Much work has been performed in motion planning, control, and cooperation across multi-independent manipulators, but recent emphasis has been given to dual-armed torsos and bi-manual cooperation and coordination. This work contributed a snap cantilever automation approach by considering and unifying three domains: intuitive assembly strategies, modular control approaches, and bi-manual control policies. In particular, the approach sought to create an approach that can generalize to assemblies of increasing geometric complexity as well as establishing the ground work for more dexterous and flexible bi-manual cantilever snap assemblies. The used strategy systematically discretizes the assembly into intuitive automata states. The latter is run in concert with scalar controllers that flexibly optimize different control objectives. These two are subject to a bi-manual coordination policy. The effectiveness of our approach was demonstrated by a bi-manual humanoid robot assembling two 4-snap cantilever parts smoothly and efficiently.**

I. INTRODUCTION

In robotic manipulation, higher levels of dexterity are sought to achieve more complex tasks with more flexibility and efficiency. Dexterity is desirable across manipulation domains including industrial, personal service, and teloperation robotics to name a few. In industrial settings, for example, market forces are driving manufacturing to shorter life cycles and more varied products. This is changing the factor from assembly lines to cell productions systems where a smaller set of skilled workers must assemble a wider variety of products requiring more dexterity and flexibility [1].

Dual arm manipulation, as part of a single body (like a humanoid robot), has been growing in interest recently. Dual arm use provides higher manipulability, innate human-form factors, high flexility and stiffness, and cost- and space-savings. [2], [3]. In particular, dual-arm robots can efficiently handle complex assemblies as they can control assembly parts' relative motion and interactions in a dexterous human-like manner.

Dual-arm humanoid robots have primarily used to study domestic applications like cooking, serving drinks, and opening appliances; also for object transport, and industrial settings such as material reshaping and gearbox assembly [2], [4]. Dual arm assembly automation requires not only to resolve traditional problems in the arm-domain like parts localization, assembly strategies, space configuration, control policies, state estimation, and failure characterization, but it must also resolve arm cooperation and coordination policies [5], including transitions from single-arm to dual-arm tasks [3]; identification of common workspace and maximally effective workspace areas [6]. Motion planning for dual-arms in real-time is complex. For this reason, the human brain selects simple trajectories that can be synchronized and monitored with ease. This leads to the classification of motions as either coordinated or uncoordinated, and as part of the former, symmetric or asymmetric [3].

This work focuses on resolving cantilever snap assembly automation. The latter are of interest since they are amply used in electronics, appliances, auto and avionics industries [7], [8]. Some work has been done in the automation of single-arm snap assemblies [9] [10], [8] but no work has yet considered snap automation using the increased dexterity provided by a dual-arm setup.

In this work, we seek to design control strategies that can generalize to geometries of increasing complexity within a class of snap fasteners with a strategy that can constraint the task to facilitate the interpretation of signals for state reasoning, while using a coordination policy that leverages the manipulability of the dual-arm system. To this end, we contribute a dual-arm assembly approach that combines that benefits of a modular control approach, an intuitive strategy that constraints the motion of the task, and a coordination policy to resolve dual-arm negotiations.

In this work, we simulated, HIRO, 6 DoF dual-arm anthropomorph robot to execute a snap assembly of a manufactured camera part consisting of 4 cantilever fixtures on its male and female parts. The fixtures are rigidly fixed to both wrists and contacts points are not explicitly modelled. An assembly strategy denominated the "Pivot Approach" (PA) was run using general task coordinates and ran in concert with modular controllers under the Control Basis framework. Furthermore, the strategy and controllers were subject to a bi-manual but asynchronous coordination policy classified as the "push-hold" scheme for the preliminary analysis of dual-arm snap assemblies. The robotic test-bed is shown in Fig. 1.

The PA was originally designed in [11] and extended here for the dual-arm case (referred to as 2PA). The PA strategy exploits snap parts' hardware design to constraint the task's

978-1-4799-7396-5/14/$31.00 © 2014 IEEE

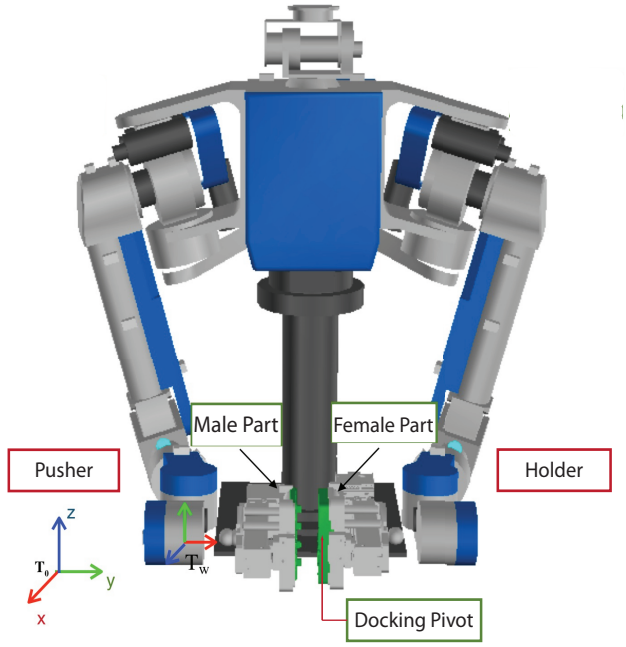

Fig. 1. The HIRO dual-arm humanoid robot, rigidly holds male and female snap camera parts that will be assembled together using a "push-hold" coordination scheme, a Pivot Approach Strategy, and a set of Control Basis controllers.

motion and generate similar sensory-signal patterns across trials. The approach systematically discretizes the assembly into intuitive automata states and facilitates pattern-encoding for state reasoning. This strategy works in concert with modular controllers that flexibly change to address multi-objective problems through null-space operations. Sets of concurrent controllers are selected for different automata states to optimize different goal sets. Furthermore, our coordination policy enacts bi-manual arm operations in a coordinated but asymmetrical and non-congruent fashion. The coordination policy is empirically derived from human examples.

Our approach though preliminary, effectively implemented the cantilever snap assembly through the established strategy, coordination policy and control framework. The FT signal-patterns displayed significantly different signature characteristics and lower overall FT levles. More importantly, this setup provides greater flexibility (the relative poses that can be used) to perform the assembly. This is significant when working with different snap pieces in industrial settings or unstructured environments for personal service or at home robots.

The rest of the paper is organized as follows: the simulation set-up is presented in Sec. II, the Control Basis Framework is presented in SEc. III, the Pivot Approach and Coordination Scheme are presented in Sec. V, Experiments and Results are presented in Sec. VI, the discussion is presented in Sec. VII, and the conclusion is presented in Sec. VIII.

II. Simulation Setup

A HIRO, 6 DoF dual-arm anthropomorph robot was simulated in the OpenHRP environment [12]. A male and female CAD rendered snap-fit camera molds were used in the Pivot Approach. The male part consisted of four snap beams, while the female part consisted of four snap-fits and a pivoting dock used to lock the male part and constraint the part's motion during the assembly. Both parts were were rigidly situated, the female part on the robot's left arm gripper and the male part on the robot's right arm gripper (see Fig.1). For simulation purposes, the pivot dock's location on the male part was provided to the system *a priori*. The tool center point (TCP) on the end-effector was chosen to be on the female part in correspondence with the male part and served as global reference for the system. The world reference frame was located at the manipulator's base. The tool point center position and orientation, were determined with reference to the world coordinate frame To. On the other hand, the force and moment reference frames were determined with respect to the wrist's reference frame Tw as in Fig. 1.

III. The Control Basis Approach

The control basis is a framework designed to flexibly but systematically build and modify controllers. This framework provides a systematic approach to building controllers, yet at the same time generalize to new situations.

The approach decomposes a control problem into a set of asymptotically stable modular control elements that can be combined and flexibly rearranged to achieve desired strategies. The framework can combine controllers through the use of a null space operator [5] and can sequentially combine primitive or compound controllers. Furthermore, the approach methodically determines which sensor inputs and motor actuators each controllers should use as well as the types of transformations necessary to transform incoming and outgoing data to the right space. The framework, in effect, builds instruction sets from a small set of basis controllers to achieve a wide range of objectives [13].

A. Mathematical Derivation

Primitive controllers ϕ_i, where $i = 1 \sim m$, are elements in a basis set of controllers, Φ, such that $\phi_i \in \Phi$. A primitive controller optimizes a partitioned portion of a designated control space (like joint angle space or cartesian force space) and can be understood as the minimization of a discrete basin of attraction. The basins of attraction are formulated through artificial potential functions defined over a typed domain, X_i, which are defined as the square of the error, where $\phi_i(\rho) = \rho^T \rho$ and ρ, is the difference between a reference input and a plant input, $\rho = \mathbf{q}_{ref} - \mathbf{q}_{des}$, at every time step.

Each controller reaches its objective by performing greedy descent, $\nabla \phi_i$, on the artificial potential function, while engaging selected sensor inputs and motor outputs. The surface potential minimization in a specified domain space, X_i, over time is defined as:

$$\nabla_{x_i} \phi_i = \frac{\partial \phi_i}{\partial t}. \quad (1)$$

Each basis controller is bound to a selected subset of sensor input resources $\gamma_j \in \Gamma_j$ and output motor resources $\gamma_k \in \Gamma_k$ relevant to the task. Input and output signals are processed through sensor transforms (*i.e.* forward kinematics), s_j, and effector transforms (*i.e.* Jacobian), e_k to ensure that a task is guaranteed to operate within the region of a corresponding basis.

The closed-loop controller is implemented then, when the error between the incoming sensor information and the reference position is minimized within the discrete artificial potential basin, $\nabla_{x_i}\phi_i(\mathbf{x}_{ref} - s_j(\Gamma_j))$, and the gradient result is mapped to the output configuration space through an effector transform, $e_k(\Gamma_l)$. Given that the input data is of the same domain type as the artificial potential function, and the effector transform is of the same dimensions as the potential function, the controller's output, $\nabla_{y_k}\phi_i$, is defined as:

$$\nabla_{y_k}\phi_i = e_k(\Gamma_l)^T \nabla_{x_i}\phi_i(\mathbf{x}_{ref} - s_j(\Gamma_j)). \quad (2)$$

For convenience, the above expression is expressed in simplified notation as $\phi_i \mid_{e_k(\Gamma_l)}^{s_j(\Gamma_j)} (\mathbf{x}_{ref})$. If the controller has zero reference, then it can be omitted: $\phi_i \mid_{e_k(\Gamma_l)}^{s_j(\Gamma_j)}$. To concurrently optimize multiple goals, secondary control updates are projected onto the nullspace of primary control updates. This relationship is expressed in a compound controller π as having the secondary controller ϕ_2 be *subject-to* the primary controller ϕ_1, and is expressed as:

$$\nabla_y(\phi_2 \triangleleft \phi_1) = \nabla_y\phi_1 + \mathcal{N}(\nabla_y\phi_1^T)\nabla_y\phi_2, \quad (3)$$

where, $\mathcal{N}(\nabla_y\phi_1^T) \equiv I - (\nabla_y\phi_1^T)^+(\nabla_y\phi_1^T)$, and *I*, is the identity matrix, *y* is an *n*-dimensional space, and the nullspace of $\nabla_y\phi_1^T$ is a (*n*-1) dimensional space orthogonal to the direction of steepest descent [4]. For convenience, Eqtn. (3) is written as $\pi_k : \phi_2 \triangleleft \phi_1$.

IV. Assembly Control Basis Set

The following primitive and compound controllers were implemented for the dual-arm 6 DoF HIRO humanoid robot. Position, force, and moment primitives are first introduced, continued by compound controller references.

A. The Position Primitive

The position controller is based on the Jacobian transpose control method, where at each cycle, joint displacements are updated according to:

$$\triangle\mathbf{q} = J^T K_p \mathbf{e}, \quad (4)$$

where, $\triangle\mathbf{q} \in \mathcal{R}^{\mathbf{7x1}}$ is a displacement of joint angles, $J^T \in \mathcal{R}^{7x6}$ is the manipulator Jacobian, $K_p \in \mathcal{R}^{7x7}$ is the position gain, and $\mathbf{e} \in \mathcal{R}^{\mathbf{6x1}}$ is the error in cartesian positions.

For the position primitive, the sensor transform s_{pr} is the identity and operates on all joints and conveniently represented as: $s_{pr}(\gamma_{joint\_pos})$. The effector transform e_{pr} is the Jacobian transpose and effects torque updates in all joint motors: $e_{pr}(\gamma_{joint})$.

The square cartesian error is used as the error function: $\phi_p = \frac{1}{2}K_p\mathbf{e}^T\mathbf{e}$, such that the gradient is $\nabla_x\phi_p = K_p\mathbf{e}$. The basis controller can thus be defined as:

$$\nabla_q\phi_p = e_{pr}(\Gamma_{joint})^T \nabla_{x_p}\phi_p(\mathbf{x}_{ref} - s_{pr}(\Gamma_I)), \quad (5)$$

or, more succinctly as $\phi_p \mid_{e_{pr}(\Gamma_{joint})}^{s_{pr}(\Gamma_I)} (\mathbf{x}_{ref})$.

Note that for our current work, a position controller was used in both the Hold and Approach stages of the 2PA (see details in Sec.V). Each controller is provided with a different trajectory point set and are referred to independently as the the *HOLD Controller* ϕ_{HOLD} and the *Approach Controller* ϕ_{APR}.

B. The Moment and Force Primitives

Two controllers, force and moment primitives, update joint angle configurations so as to apply desired forces or moments. The force controller updates the end-effecter's location while the moment controller updates its pose.

$$\triangle\mathbf{q_{1-7}} = K_j^{-1}J^T K_f(\mathbf{f}_{ref} - \mathbf{f}), \quad (6)$$

$$\triangle\mathbf{q_{1-7}} = K_j^{-1}J^T K_m(\mathbf{m}_{ref} - \mathbf{m}), \quad (7)$$

where, $(\mathbf{f}_{ref} - \mathbf{f})$ and $(\mathbf{m}_{ref} - \mathbf{m})$ are the force and moment errors conformed by the first three and last three elements in a $\mathcal{R}^{6x1}$ vector respectively; and, K_f and K_m are the diagonal elements of a positive definite matrix $\mathcal{R}^{6x6}$ that multiplied by the Jacobian transpose $J^T \in \mathcal{R}^{7x6}$ generate torque updates for the appropriate joint configurations. The inverse of K_j and the other gains are precomputed to generate corresponding joint angle updates for each control cycle.

The force and moment residual controllers have sensor transforms $s_{fr}(\gamma_{force})$ and $s_{mr}(\gamma_{moment})$ that return the F/T sensor data respectively. The artificial potential functions for the force and moment residual functions are proportional to the square of their errors:

$$\phi_{fr} = \frac{1}{2}K_f(\mathbf{f}_{ref} - \mathbf{f})^2, \quad \phi_{mr} = \frac{1}{2}K_m(\mathbf{m}_{ref} - \mathbf{m})^2, \quad (8)$$

and they are differentiated with respect to their joint angle configurations to displace the trusses and minimize residuals:

$$\nabla_q\phi_{fr} = -K_f(\mathbf{f}_{ref} - \mathbf{f}), \quad \nabla\phi_{mr} = -K_m(\mathbf{m}_{ref} - \mathbf{m}). \quad (9)$$

The controllers also have effector transforms $e_{fr}(\gamma_{torque})$ and $e_{mr}(\gamma_{torque})$ that converts appropriate force updates into joint torque updates by multiplying the inverse position gains and Jacobian transpose: $e_{fr}(\gamma_{torque}) = K_j^{-1}(J_{\gamma_1}, ..., J_{\gamma_{|\Gamma_k|}})^T$ and $e_{mr}(\gamma_{torque}) = K_j^{-1}(J_{\gamma_1}, ..., J_{\gamma_{|\Gamma_l|}})^T$ to produce the following primitive controllers:

$\phi_{mr} \mid_{e_{mr}(\gamma_{torque})}^{s_{mr}(\gamma_{moment})}$:

$$\nabla_q\phi_{mr} = e_{mr}(\gamma_{torque})^T \nabla_m\phi_{mr}(\mathbf{m}_{ref} - s_{mr}(\gamma_{moment})). \quad (10)$$

$\phi_{fr} \mid_{e_{fr}(\gamma_{torque})}^{s_{fr}(\gamma_{force})}$:

$$\nabla_q\phi_{fr} = e_{fr}(\gamma_{torque})^T \nabla_f\phi_{fr}(\mathbf{f}_{ref} - s_{fr}(\gamma_{force})). \quad (11)$$

C. Pivot Controller

The Pivot Controller π_{PIV} is a compound FT controller with a dominant force controller ϕ_{fr} and a subordinate moment controller ϕ_{mr}. The controller's subordinate update commands are projected unto the nullspace of the dominant controller's update space to optimize both objectives. The force controller uses a reference parameters to push towards the female part $\hat{x}_w$ as well as towards the female part's anterior wall $\hat{z}_w$: such that $\mathbf{f}_{ref} = \{6.5, 0, -13.85\}$N. As for ϕ_{mr}, its reference parameter applies a torque about the pitch axis ($\hat{y}_W$) $\mathbf{m}_{ref} = \{0, 60, 0\}$Nm.

D. Insertion Controller

The compliant insertion controller π_{CI} in this case has the same structure as the Pivot Controller pi_{PIV} and the same reference force. However, the reference moment is increased in magnitude as the posterior male-snap make contact with the female part. The increased moment is designed to push the snaps in, as the parts slides in smoothly given that all inner wall-linings are correctly aligned. The reference moment here is set to $\mathbf{m}_{ref} = \{0, 75, 0\}$Nm.

E. Mating Controller

The last controller is the mating controller π_{MAT} is a composite force-position controller that uses a dominant force controller to maintain the mating position achieved upon contact during with the male's part back wall while the subordinate position controller seeks to maintain the position detected at contact. The mating controller is defined in Eqtn. 12.

$$\pi_{MAT} = \phi_{fr} \,|^{s_{fr}(\gamma_{joint\_pos})}_{e_{fr}(\gamma_{torque})}\, (\mathbf{f}_{ref}) \triangleleft \phi_p \,|^{s_{pr}(\gamma_{force})}_{e_{pr}(\gamma_{torque})}\, (\mathbf{p}_{ref}). \tag{12}$$

V. The Pivot Approach Strategy

The Pivot Approach was originally designed generalizable state and transition conditions that can be applied to differing geometries of the snap-fit class [8]. In this work, the strategy has been extended to provide for a dual-arm setting.

To do so, the strategy must now work in tandem with a coordination policy. In [3], Kruger *et al.* present an overview of possible coordination schemes for dual-arm humanoid robots. In the presence of dual-arms, robots can control not only the relative motion of assembly parts but their interaction as well. Dual-arms can perform uncoordinated or coordinated motions. The former refers to tasks in which arms are independent of each other, while the latter refers to motions that have spatio-temporal relations. Coordinated motions are further subdivided into goal coordinated motions and bi-manual operations. The former refers to tasks where both arms achieve a goal but do not interact with each other such as typing on keyboard. Bi-manual operations on the other hand, form a closed kinematic-chain between the two arms at contact point. Bi-manual tasks can group arm motion into symmetric or asymmetric movements. Within bi-manual tasks [3] further classified a common set of elemental actions: approach/retract, grasp/release, insert/extract, slide, hold, move, yield, and hinge. These actions span the action space required for simple geometrical shapes.

Cantilever snap assemblies, can have complex geometrical configurations, specially when the number of snaps is 2 or higher. These parts contain interior wall-linings that assist in part's mating. A pivoting dock is usually located on the manufactured pieces' edge where the front wall's top edge bisects the snaps' plane of symmetry (see Fig. 1). To simplify the assembly, constrain the motion, and promote similar signal-patterns across trials, a bi-manual pivoting motion is used as part of our scheme. The complete state sequence is now introduced.

The bi-manual Pivot Approach is composed of four compound states. Each state is coupled with an action for each of the two arms. As mentioned early, bi-manual tasks can be performed in symmetrical or asymmetrical ways. For the purposes of snap assembly, a symmetrical operation implies having both arms pivoting and driving the insertion simultaneously, while the asymmetrical operation implies having one arm rigidly holding a part, while the other arm drives the insertion. In this work, we only considered the asymmetrical approach. Assuming both arms are rigidly holding the parts, the left arm functions as a rigidly holding arm, while the right arm inherits the PA strategies of the single-arm task. Additionally, this work does not explicitly consider the optimization of the pose of both arms, which is left for future work. Hence, both arms commence from their home positions as illustrated in Fig. 1, and begin the assembly with an Approach-Hold state, followed by a Pivot-Hold state, followed by an Insertion-Hold state, and finalizes with a Mating-Hold state. The state machine is shown in Fig. 2. From the homing position in the Approach State, the left holding arms will implement a primitive position controller (discussed in Sec. III) ϕ_{HOLD} with high stiffness at a pose that facilitates the pivoting motion of the male arm. The ϕ_{HOLD} controller runs while the right arm transitions through the four automata states mentioned earlier. For the right pushing arm, the strategy begins by calling a primitive position controller ϕ_{APR} that follows a smooth curved trajectory towards the docking position's neighboring area. The trajectory as in the single-arm case seeks to keep the male part's base normal collinear but in the opposite direction with the female part's base normal. For the dual arm case, Such pose has both wrists the pose of the wrists and snap parts are symmetrical to each other about the sagittal ($y = 0$) plane. As the male part approaches the female part, the trajectory slows down and seeks to make contact at an angle α. This facilitates the pivoting motion of the next state. α can vary between: $0 \leq \alpha \leq \pi/2$ while ensuring no joint limits are violated. Smaller angles are preferable as they speed up the completion of the following automata state (we used $\alpha = \pi/8$). The transition condition contains a force threshold along the normal ($-\hat{y}_o$) direction of the female base. Once this threshold is met, the strategy continues with the Pivoting State, π_{PIV}. The pivot controller applies a moment about

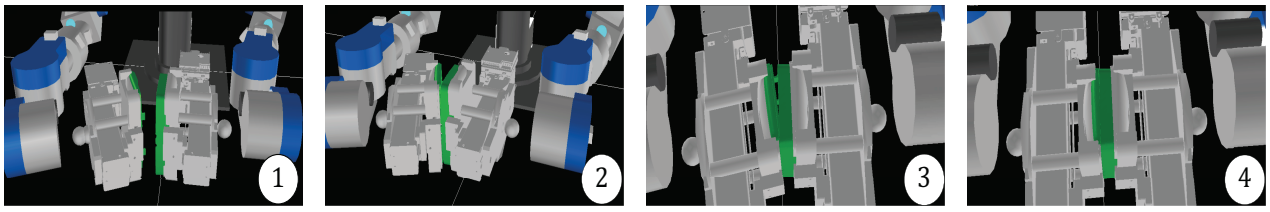

(a) Approach-Hold State (b) Pivot-Hold State. (c) Insertion-Hold State. (d) Mating-Hold State

Fig. 3. The Bi-manual Pivot Approach under a "push-hold" scheme is composed of four compound states as shown above.

the pivot axis ($\hat{z}_o$) in incremental steps until contact is made with the snaps and a Pitch angle threshold is exceeded. This position is near optimal for insertion. The insertion controller π_{CI} applies a moment along the ($\hat{z}_w$) direction, until parts reach a mating state which is checked through a combined force and joint position threshold. Finally, the Mating State activates, the mating controller π_{MAT} to maintain a coupled position and steady contact forces between the parts.

VI. Experiments

For our experiments, we tasked the dual-arm 6 DoF humanoid robot HIRO to perform a bi-manual cantilever snap assembly with a pair of male and female snap parts shown in Fig. 1. By running the 2PA under a select set of basis controllers described in Sec. III and a "push-hold" coordination policy described in Sec. V the robot effectively performed the cantilever snap assembly using both arms. Fig 3 shows four snapshots depicting each of the four automata states in the strategy.

In our simulation, the world reference frame was located at the manipulator's base. The tool point center position and orientation, were determined with reference to the world coordinate frame To. On the other hand, the force and moment reference frames were determined with respect to the wrist's reference frame Tw as in Fig. 1.

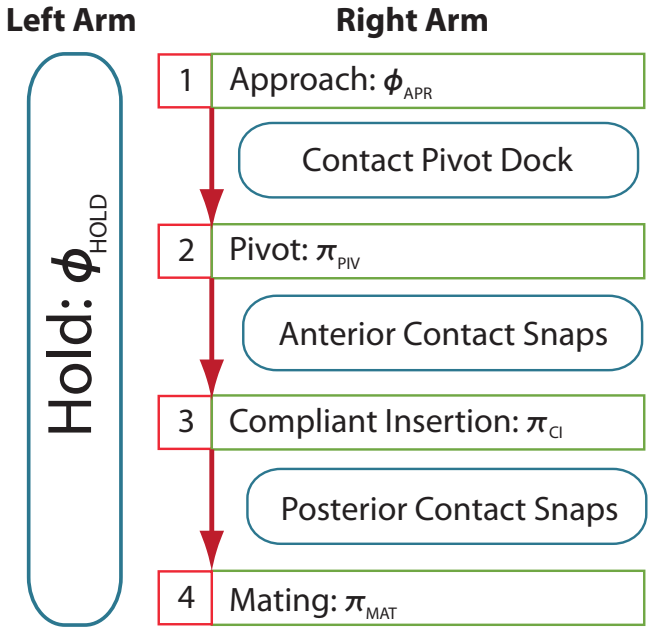

Fig. 2. Finite state machine for the Bi-manual Pivot Approach strategy under a "push-hold" scheme.

A. Results

Our strategy led to the force-torque signatures seen in Fig. 4. In this next part we present an analysis of the graph and comment on its similarities and differences to the one-hand approach. The Approach trajectory of the arm initially shows a small change in forces and moments exerted by the initial arm acceleration from the homing position. The forces and moments settle as the arm moves with constant velocity. Upon arriving at the docking pivot, a small abrupt change in the force and moment signatures is registered. This contact signals the commencement of the Pivot State. In the latter, forces in the wrist's x- and z-direction are trying to maintain a constant profile. These constant signatures, however, become disrupted towards the end of this state(around 10-12 seconds) due to contact by the male and female posterior snaps. On the other hand, F_y, M_x, and M_z register negligible changes as the constrained assembly motion restricts movements away from the pitch rotation axis. Finally, M_y, experiences a constant moment until the 10 second marker where, as mentioned earlier, the posterior snaps begin to make contact. Between the Pivot and Insertion stages there is in effect a transition window, where force and moment signatures become noisy about M_y. This is due to the snap's elastic nature. As the snaps on the posterior side make contact they go through an accommodation period in order to begin sliding in place. Next is the Insertion State, in which the parts are at optimal position for the final snap in place. Large variations are registered across all states, but particularly around the 15th second. The snapping motion is abrupt and has a tangible effect in all six DoF.

VII. Discussion

The current research effectively implemented cantilever snap assemblies using a dual-arm humanoid robot by combining the benefits of the flexible and modular control basis approach, a coordination policy to resolve dual-arm negotiations, and a flexible intuitive strategy that constrains the task's motion to facilitate state estimation. The results is important in a number of ways. It provides an example of an implementation for snap assemblies using bi-manipulation, that does not seems to exist in the literature. It also, while preliminary, sets the ground work to expand the dexterity of the robot by allowing it to implement these assemblies not just at a fixed location in the workspace, but at a variety

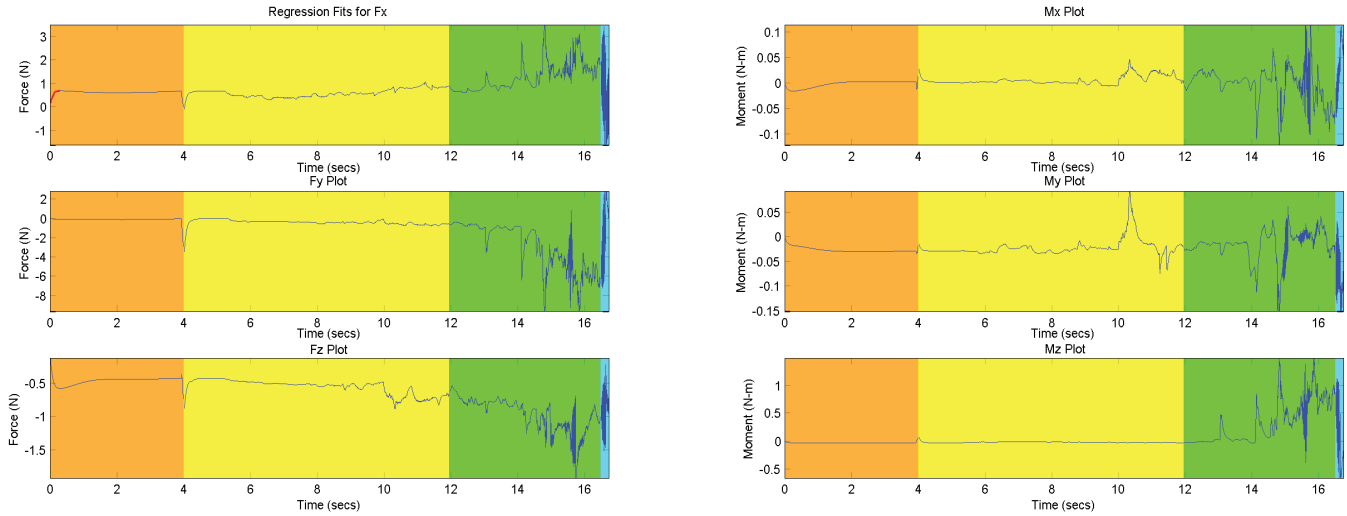

Fig. 4. Force and Moment signatures for the right arm FT sensor. The orange, yellow, green, and blue colors represent the four automata states.

of poses in the reachable area of both arms. Furthermore the flexibility and modularity of our work, as it pertains to the problem of cantilever snap assemblies, is useful as it permits our approach to generalize to different cantilever parts of increasing geometric complexity as it was shown in [8]. Kruger *et al.* performed a similar work. Their focus attends manipulation tasks of greater generality than the snap assembly problem, however, it seems their control approach is not as flexible as their strategy to adapt to tasks with different control objectives as referred to in Sec. III. Besides this example, most research works have focused on considering only the strategy, or the control problem, or the coordination policy, independently [2].

Some of the limitations of our work are related to its heuristic nature. Learned approaches for the strategy and the coordination policies would render the work more generalisable to different scenarios. Our approach has also not considered contact states or internal forces. The authors were surprised to record FT signatures that were much smoother than those for the single arm case. An analysis of these dynamics should be undertaken. As part of our future work, we will endeavour to study learned strategies, policies, and state estimation techniques that can aid in the generalization of the work. Additionally, we need to design a policy to effect snap assemblies with the least energy within the union of the workspace of the arms. Finally, we would like to also design automated policies that permit a robot to transition between two-arm activity and single-arm activity in a natural way.

VIII. CONCLUSION

In this work, snap cantilever automation was sought by combining a flexible and intuitive assembly strategy, with a similarly flexible and modular control basis framework, along with a "push-hold" coordination policy. The approach sought both to create an approach that can generalize to assemblies of increasing geometric complexity as well as establishing the ground work for more dexterous and flexible bi-manual cantilever snap assemblies.

REFERENCES

[1] H. M. Do, C. Park, and J. H. Kyung, "Dual arm robot for packaging and assembling of it products," in *Automation Science and Engineering (CASE), 2012 IEEE International Conference on*. IEEE, 2012, pp. 1067–1070.

[2] C. Smith, Y. Karayiannidis, L. Nalpantidis, X. Gratal, P. Qi, D. V. Dimarogonas, and D. Kragic, "Dual arm manipulationa survey," *Robotics and Autonomous Systems*, vol. 60, no. 10, pp. 1340 – 1353, 2012. [Online]. Available: http://www.sciencedirect.com/science/article/pii/S092188901200108X

[3] J. Krger, G. Schreck, and D. Surdilovic, "Dual arm robot for flexible and cooperative assembly," {*CIRP*} *Annals - Manufacturing Technology*, vol. 60, no. 1, pp. 5 – 8, 2011. [Online]. Available: http://www.sciencedirect.com/science/article/pii/S0007850611000187

[4] R. J. Platt, "Learning and generalizing control-based grasping and manipulations skills," Ph.D. dissertation, U. of Mass. Amherst, 2006.

[5] J. Rojas and R. P. II, "Analysis of autonomous cooperative assembly using coordination schemes by heterogeneous robots using a control basis approach," *J. of Autonomous Robots*, vol. 32, no. 2, pp. 97–172, 2012.

[6] Y. Guan, K. Yokoi, and X. Zhang, "Numerical methods for reachable space generation of humanoid robots," *The International Journal of Robotics Research*, vol. 27, no. 8, pp. 935–950, 2008.

[7] J. Camillo, *Snap Fits Enable Plastic Parts Assembly*, Assembly Magazine Std., April 2014. [Online]. Available: http://www.assemblymag.com/articles/92047-snap-fits-enable-plastic-parts-assembly

[8] J. Rojas, K. Harada, H. Onda, N. Yamanobe, E. Yoshida, K. Nagata, and Y. Kawai, "Towards snap sensing," *International Journal of Mechatronics and Automation*, vol. 3, no. 2, pp. 69–93, 2013.

[9] A. Stolt, M. Linderoth, A. Robertsson, and R. Johansson, "Force controlled assembly of emergency stop button," in *IEEE Int'l Conf. on Robotics & Automation*, 2011.

[10] K. S. Chin, M. M. Ratnam, and R. Mandava, "Force-guided robot in automated assembly of mobile phone," *J. of Assembly & Aut.*, vol. 23, no. 1, pp. 75–86, 2003.

[11] J. Rojas, K. Harada, H. Onda, N. Yamanobe, E. Yoshida, K. Nagata, and Y. Kawai, "Cantilever snap assembly automation using a constraint-based pivot approach," in *IEEE Intl. Conf. on Mechatr. & Automation*, 2012.

[12] F. Kanehiro, H. Hirukawana, and S. Kajita, "Openhrp: Open architecture humanoid robotics platform," *Intl. J. of Robotics Res.*, vol. 23, no. 2, pp. 155–165, 2004.

[13] O. Brock, A. Fagg, R. Grupen, R. Platt, M. Rosenstein, and J. Sweeney, "A framework for learning and control in intelligent humanoid robots," *Intl. J. of Humanoid Robots*, vol. 2, no. 3, pp. 301–336, 2005.